

Measurement of the $e^+e^- \rightarrow Z \rightarrow b\bar{b}$ Forward-Backward Asymmetry and the $B^0\bar{B}^0$ Mixing Parameter Using Prompt Leptons

The L3 Collaboration

Abstract

The time-integrated $B^0\bar{B}^0$ mixing parameter and the forward-backward charge asymmetry in the process $e^+e^- \rightarrow b\bar{b}$ are measured in hadronic Z events containing prompt muons or electrons, collected by the L3 experiment in the years 1990 to 1995. The total sample of 3.3 million hadronic Z events with a mean centre-of-mass energy of 91.26 GeV yields:

$$\begin{aligned} A_{\text{FB}}^b &= 0.0960 \pm 0.0066(\text{stat.}) \pm 0.0033(\text{sys.}), \\ \chi_b &= 0.1192 \pm 0.0068(\text{stat.}) \pm 0.0051(\text{sys.}). \end{aligned}$$

This asymmetry measurement together with measurements at energies away from the Z pole energy yield a pole asymmetry and corresponding effective electroweak mixing angle of:

$$\begin{aligned} A_{\text{FB}}^{0,b} &= 0.1015 \pm 0.0064(\text{stat.}) \pm 0.0035(\text{sys.}), \\ \sin^2 \bar{\theta}_W &= 0.2318 \pm 0.0013. \end{aligned}$$

Submitted to *Phys. Lett. B*

Introduction

In the process $e^+e^- \rightarrow Z \rightarrow b\bar{b}$, the distribution of the quark production angle θ_b relative to the electron beam direction can be parametrised by:

$$\frac{d\sigma}{d \cos \theta_b} \propto \frac{3}{8}(1 + \cos^2 \theta_b) + A_{\text{FB}}^b \cos \theta_b.$$

Within the Standard Model [1] for lowest order Z exchange, at $\sqrt{s} = m_Z$, the forward-backward pole asymmetry $A_{\text{FB}}^{0,b}$ is related to the vector v_f and axial-vector a_f couplings of fermions to the Z boson by:

$$A_{\text{FB}}^{0,b} = \frac{3}{4} \frac{2v_e a_e}{v_e^2 + a_e^2} \frac{2v_b a_b}{v_b^2 + a_b^2}. \quad (1)$$

Higher order corrections are accounted for by replacing the couplings v_f, a_f with modified effective couplings \bar{v}_f, \bar{a}_f [2] which are related by:

$$\frac{\bar{v}_f}{\bar{a}_f} = 1 - 4|q_f| \sin^2 \bar{\theta}_W, \quad (2)$$

where q_f is the fermion charge and $\bar{\theta}_W$ is the effective electroweak mixing angle.

The high sensitivity of the down type quark asymmetries to $\sin^2 \bar{\theta}_W$ and the relative ease of selecting pure $Z \rightarrow b\bar{b}$ samples make A_{FB}^b measurements excellent tests of Standard Model predictions.

Due to mixing in the $B^0\bar{B}^0$ system where a B_d^0 or B_s^0 oscillates into its anti-particle the observed asymmetry is diluted by a factor $1/(1-2\chi_b)$, where χ_b is the mixing parameter. In the Standard Model the oscillation proceeds by a weak flavour-changing box diagram, dominated by virtual top-quark exchange. The rate of mixing depends on the Cabibbo-Kobayashi-Maskawa matrix elements, V_{td} and V_{ts} , the top-quark mass and the B meson decay constant.

Electrons and muons from the semileptonic decays of b-quarks are used to select events coming from $Z \rightarrow b\bar{b}$. The large mass and hard fragmentation of the b-quark results in prompt leptons from b-quark decays having high momentum p and transverse momentum p_t with respect to the quark direction; the p_t reflects the momentum distribution in the centre-of-mass frame of the heavy hadron. Thus, a high p, p_t lepton within a jet provides both b-flavour enhancement and charge information, from the correlation of the lepton charge, q , with the quark charge. The quark direction estimator is obtained from the event thrust axis. Prompt leptons constitute roughly 1% of all charged particles produced in hadronic events. Thus, both effective background rejection and lepton selection are required.

Events containing two high p, p_t leptons in different jets allow the rate of mixing to be determined. As both oscillations from B_d^0 and B_s^0 mesons contribute to the observed mixing, $\chi_b = f_d\chi_d + f_s\chi_s$, where f_d and f_s are the production fractions of B_d^0 and B_s^0 mesons.

In this paper, measurements of A_{FB}^b and χ_b with the L3 detector [3], using events collected at centre-of-mass energies, \sqrt{s} , close to the Z pole energy during the data taking periods of 1993-1995, are presented. The data sample consists of 2.3 million hadronic events with mean energy 91.24 GeV. Measurements using data collected during 1993-1995 at centre-of-mass energies significantly below and above the pole energy are also presented. These measurements are combined with previous L3 results [4] using data from the 1990-1992 running periods, corresponding to 1.04 million hadronic events. The combined result is used to extract a value for the effective weak mixing angle $\sin^2 \bar{\theta}_W$. Other LEP measurements of these quantities are reported in References [5-8].

Event selection

A detailed description of the L3 detector is provided by Reference [3]. The trigger requirements and the selection criteria for hadronic events containing electrons or muons have been described previously [9,10]. Muons are identified and measured in the muon chamber system. We require that a muon track consists of track segments in at least two of the three layers of muon chambers, and that the muon track points back to the interaction region. Electrons are identified using the electromagnetic and hadronic calorimeters, as well as the central tracking chamber. Only electrons in the barrel region $|\cos \theta| < 0.69$ are considered for this analysis. Requiring less than 3 GeV to be deposited in a cone of half angle 7° behind the electromagnetic cluster rejects hadrons which fulfil the electron shower shape and energy criteria in the electromagnetic calorimeter. Photons are rejected by requiring a track in the central tracking chamber to be matched with the electromagnetic cluster. The track curvature in the central tracking chamber determines the charge of the electron. The electron selection, in particular the shower shape criteria, implies an isolation requirement on identified electrons. This results in a lower efficiency for electrons than for muons.

The momentum of muon candidates is required to be greater than 4 GeV, while the electron candidates are required to have momentum greater than 3 GeV. Requirements on the transverse momentum $p_t > 1$ GeV of the leptons are used to further enhance the $b\bar{b}$ purity. The transverse momentum is defined with respect to the nearest jet, where the measured momentum of the lepton is excluded from the jet. If there is no jet with an energy greater than 6 GeV in the same hemisphere as the lepton, the p_t is calculated relative to the thrust axis of the event. In events containing more than one lepton candidate, only the highest p_t lepton is used in the asymmetry analysis.

For the mixing determination, two leptons are required with a separation angle of more than 60° to provide tagging information from two b-hadrons originating from different jets. The transverse momenta of the leptons are required to be greater than 0.5 GeV. In events containing more than two leptons the two with the highest transverse momentum are considered.

After hadron selection and detector quality requirements the total number of hadronic events selected is 2.3 million, at a mean centre-of-mass energy of 91.24 GeV. Of these, the number with prompt lepton candidates selected is 79417, comprising 55597 with muon candidates and 23820 with electron candidates. The number of dilepton events selected, after all cuts is 4452, comprising 2046 muon-muon candidates, 1874 muon-electron candidates and 532 electron-electron candidates.

Event simulation

The JETSET 7.4 Monte Carlo program [11] is used to generate event samples, simulating the fragmentation and decay of hadronic events. The events are passed through the full L3 detector simulation [12], which includes the effects of experimental resolution, energy loss, multiple scattering, interactions and decays in the detector materials.

Relevant electroweak parameters, fragmentation parameters, semileptonic decay models, and branching ratios are set to their current best values and the uncertainties on these parameters are used to determine the systematic uncertainties on the results. The parameter values and variations follow the recommendations developed in Reference [13] and updated in Reference [14]; and are summarised below together with the resulting systematic uncertainties on A_{FB}^b and χ_b .

The distributions of the scaled energy ($x_E = 2E_{\text{hadron}}/\sqrt{s}$) of weakly decaying heavy hadrons are modelled using the Peterson fragmentation function [15]. The shape determining Peterson parameters ϵ_b, ϵ_c for b and c hadrons are adjusted to attain the recommended mean scaled energies $\langle x_E(b) \rangle$ and $\langle x_E(c) \rangle$. The lepton momentum spectra implemented in JETSET are re-weighted using several models, adjusting the spectra for both the ‘central point’ at which the measurement is made as well as the ‘upper’ and ‘lower’ points used to determine the systematic uncertainties. The sign convention used is for the harder and softer spectra to be modelled by the upper and lower points, respectively. For $b \rightarrow \ell$ decays the ACCMM model [16] with Fermi momentum $p_f = 298$ MeV and produced c-quark mass 1673 MeV is used as the central point, and the ISGW model [17] with 11% D^{**} and 32% D^{**} (ISGW **) are used as upper and lower points of the systematic variation. For $c \rightarrow \ell$ decays the ACCMM model is used as a convenient functional form, with parameters for the central point and variations chosen from fits to DELCO [18] and MARK III [19] data. For the $b \rightarrow c \rightarrow \ell$ decay chain, the $b \rightarrow D$ spectrum measured by CLEO [20] is combined with the $c \rightarrow \ell$ spectrum corrected by the procedure described above.

Monte Carlo events with single leptons, or the highest p_t lepton in multi-lepton events, are classified into six categories: $b \rightarrow \ell$, $b \rightarrow c \rightarrow \ell$, $b \rightarrow \tau \rightarrow \ell$, $b \rightarrow \bar{c} \rightarrow \ell$, $c \rightarrow \ell$ and background. Where the class $b \rightarrow \bar{c} \rightarrow \ell$ represents the cascade $b \rightarrow W \rightarrow \bar{c} \rightarrow \ell$. The background includes leptons from π and K decays, Dalitz decays, photon conversions and misidentified hadrons. Examples of the causes of misidentifying hadrons as leptons are $\pi - \gamma$ overlaps for electrons and punchthrough for muons. The Monte Carlo estimate of the sample composition is shown in Table 1 together with the asymmetry contribution of each source.

Simulated events with two leptons separated by more than 60° are classified into eight categories, listed in Table 2 together with the estimated sample composition.

Asymmetry Determination

The observed asymmetry is extracted by applying an unbinned maximum-likelihood fit to the p and p_t distributions, assuming no $B^0\bar{B}^0$ mixing. The likelihood function has the form:

$$\mathcal{L} = \prod_{i=1}^{N_{\text{data}}} \sum_{k=1}^6 f_k(i) \cdot \left[\frac{3}{8}(1 + \cos^2 \theta_i) + A_k \cos \theta_i \right].$$

For each data lepton i the fractions in each category k , $f_k(i)$, are determined from the number and type of Monte Carlo leptons found within a rectangular box centered on the data lepton in the p - p_t plane. The box dimensions are increased until a minimum of 30 Monte Carlo leptons are included in the box. The six categories are listed in Table 1 together with their associated asymmetries A_k . The estimate of the b-quark direction $\cos \theta_i$ is obtained from the observable $-q \cos \theta_T$, where the thrust direction θ_T is oriented into the hemisphere containing the lepton, of charge q . Figures 1 and 2 show the p , p_t and $-q \cos \theta_T$ distributions for the selected electrons and muons together with the predicted Monte Carlo fractions of the various sources.

Extraction of the Mixing Parameter

A maximum-likelihood fit, described in detail in Reference [10], is used to extract the mixing parameter. The probability functions for the two leptons to come from various sources are assumed to factorize, allowing the functions to be determined independently from single lepton

Monte Carlo events by counting the number and type of Monte Carlo leptons found in (p_l, p_t) boxes, where p_l is the lepton momentum along the jet axis.

A global probability function, with terms representing each of the different sign combinations of the two leptons, is constructed from the single lepton probability functions and several parameters, namely α , which is the fraction of $b\bar{b}$ events in the dilepton sample, β , the fraction of (u,d,s,c) with opposite charges in the dilepton sample, B , the fraction of $b \rightarrow \ell$ events in the total b decay sample and $C(p_1, p_2)$ which takes into account possible correlations between the lepton momenta.

Parameters α , β and B are evaluated from the Monte Carlo sample and are fixed in the fit ($\alpha = 0.813$, $\beta = 0.070$, $B = 0.705$). The contribution of these parameters to the systematic uncertainties are evaluated by a 2 % variation around the fixed values, corresponding to the estimated error on the value. As Monte Carlo studies have shown that the correlation parameter C is compatible with zero, it is fixed at zero in the fit.

Figure 3 shows the stability of χ_b as a function of the minimum transverse momentum of the two leptons. Results from the maximum-likelihood fit are compared with results from a simple counting method [10], used as a cross-check.

Results

The A_{FB}^b results from the 1993-1995 data sample at the Z peak, with an average centre-of-mass energy of 91.24 GeV, and the χ_b results from all energy points are:

$$\begin{aligned} A_{\text{FB}}^b &= 0.0977 \pm 0.0080(\text{stat.}) \pm 0.0033(\text{sys.}) \\ \chi_b &= 0.1172 \pm 0.0083(\text{stat.}) \pm 0.0051(\text{sys.}) \end{aligned}$$

The observed asymmetry is corrected for the effects of mixing using the reported χ_b value and the A_{FB}^b uncertainties take account of correlations between the systematics of the mixing and observed asymmetry determinations.

Details of the systematic uncertainties are provided in Table 3, including dependencies on other electroweak parameters; the parameter values and variations are listed. The electroweak parameters varied include the ratios of the b and c quark partial widths of the Z to its total hadronic partial width, R_b and R_c , as well as the forward-backward asymmetry of c quarks, A_{FB}^c ; the values and variations used correspond to the world average results reported in Reference [21]. Separate fits for muons and electrons are performed, yielding consistent results. Estimates of the charge confusion for muons and electrons are made and corrections are applied. The error on the charge confusion estimate is included as a contribution to the systematic error.

Effects of reconstruction uncertainties in the simulation of the lepton momentum and in the jet direction determination are estimated by smearing the lepton momentum by 2% and the angle between the lepton and the nearest jet by 1°. Monte Carlo studies show the background asymmetry to be consistent with zero, we vary this by ± 0.01 as an estimate of the uncertainty on this quantity.

The results for A_{FB}^b , from the peak data alone, and χ_b are combined with the 1990-1992 results [4] to yield:

$$\begin{aligned} A_{\text{FB}}^b &= 0.0960 \pm 0.0066(\text{stat.}) \pm 0.0033(\text{sys.}) \\ \chi_b &= 0.1192 \pm 0.0068(\text{stat.}) \pm 0.0051(\text{sys.}) \end{aligned}$$

from the total sample of 3.3 million hadronic Z decays. The data is divided into energies below, on and above the Z resonance due to the centre-of-mass energy dependence of A_{FB}^b , as illustrated in Table 4 and Figure 4. The results after applying QCD corrections, to remove the diluting effects of QCD, are compared with the Standard Model predictions of ZFITTER [22] with QCD effects removed. The Standard Model parameters used correspond to $\sin^2 \bar{\theta}_W = 0.2315$. In performing the combination it was necessary to re-evaluate some systematic uncertainties from the 1990-92 analysis to account for significant non-linear behaviour of the uncertainties as a function of the input parameters, particularly for $\text{Br}(b \rightarrow \ell)$.

Determination of $\sin^2 \bar{\theta}_W$

In order to convert the three measured asymmetries A_{FB}^b to a pole asymmetry $A_{\text{FB}}^{0,b}$ or equivalently $\sin^2 \bar{\theta}_W$, corrections to account for the centre-of-mass energy dependence are applied to the off-peak points, allowing a combination with the peak point. Further small corrections are applied to account for QED and QCD effects as well as effects from the centre-of-mass energy dependence, as described in Reference [13]. The event selection bias s_b and QCD correction factor C_b , defined by:

$$A_{\text{FB}}^b = (1 - s_b \times \delta_{\text{QCD,ref}}^{\text{had,T}}) A_{\text{FB}}^{0,b} = (1 - C_b) A_{\text{FB}}^{0,b},$$

are obtained from Monte Carlo and generator level studies to be $s_b = 0.72 \pm 0.12(\text{stat.})$ and $C_b = (2.07 \pm 0.36(\text{stat.}) \pm 0.24(\text{th.}))\%$, where the reference value $\delta_{\text{QCD,ref}}^{\text{had,T}}$ is determined to be $(2.87 \pm 0.35)\%$ using the results of analytic calculations at parton level corrected by generator studies of the effects of hadronisation. Full details of the determination of the QCD correction applied to this analysis are provided in Reference [23].

Equations 1 and 2 are used to relate the pole asymmetry $A_{\text{FB}}^{0,b}$ to $\sin^2 \bar{\theta}_W$, yielding results from the full 1990-1995 data sample:

$$\begin{aligned} A_{\text{FB}}^{0,b} &= 0.1015 \pm 0.0064(\text{stat.}) \pm 0.0035(\text{sys.}), \\ \sin^2 \bar{\theta}_W &= 0.2318 \pm 0.0013. \end{aligned}$$

The results are compatible with previous L3 and LEP measurements, and are consistent with Standard Model expectations.

Acknowledgments

We wish to express our gratitude to the CERN accelerator divisions for the excellent performance of the LEP machine. We acknowledge the contributions of all the engineers and technicians who have participated in the construction and maintenance of this experiment.

The L3 Collaboration:

M. Acciarri,²⁷ P. Achard,¹⁹ O. Adriani,¹⁶ M. Aguilar-Benitez,²⁶ J. Alcaraz,²⁶ G. Alemani,²² J. Allaby,¹⁷ A. Aloisio,²⁹ M.G. Alviggi,²⁹ G. Ambrosi,¹⁹ H. Anderhub,⁴⁸ V.P. Andreev,^{7,37} T. Angelescu,¹³ F. Anselmo,¹⁰ A. Arefiev,²⁸ T. Azemoon,³ T. Aziz,¹¹ P. Bagnaia,³⁶ L. Baksay,⁴³ A. Balandras,⁴ R.C. Ball,³ S. Banerjee,¹¹ Sw. Banerjee,¹¹ K. Banicz,⁴⁵ A. Barczyk,^{48,46} R. Barillere,¹⁷ L. Barone,³⁶ P. Bartalini,²² M. Basile,¹⁰ R. Battiston,³³ A. Bay,²² F. Becattini,¹⁶ U. Becker,¹⁵ F. Behner,⁴⁸ J. Berdugo,²⁶ P. Berges,¹⁵ B. Bertucci,³³ B.L. Betev,⁴⁸ S. Bhattacharya,¹¹ M. Biasini,³³ A. Biland,⁴⁸ G.M. Bilei,³³ J.J. Blaising,⁴ S.C. Blyth,³⁴ G.J. Bobbink,² R. Bock,¹ A. Böhm,¹ L. Boldizar,¹⁴ B. Borgia,^{17,36} D. Bourilkov,⁴⁸ M. Bourquin,¹⁹ S. Braccini,¹⁹ J.G. Branson,³⁹ V. Brigljevic,⁴⁸ F. Brochu,⁴ I.C. Brock,³⁴ A. Buffini,¹⁶ A. Buijs,⁴⁴ J.D. Burger,¹⁵ W.J. Burger,³³ J. Busenitz,⁴³ A. Button,³ X.D. Cai,¹⁵ M. Campanelli,⁴⁸ M. Capell,¹⁵ G. Cara Romeo,¹⁰ G. Carlino,²⁹ A.M. Cartacci,¹⁶ J. Casaus,²⁶ G. Castellini,¹⁶ F. Cavallari,³⁶ N. Cavallo,²⁹ C. Cecchi,¹⁹ M. Cerrada,²⁶ F. Cesaroni,²³ M. Chamizo,²⁶ Y.H. Chang,⁵⁰ U.K. Chaturvedi,¹⁸ M. Chemarin,²⁵ A. Chen,⁵⁰ G. Chen,⁸ G.M. Chen,⁸ H.F. Chen,²⁰ H.S. Chen,⁸ X. Chereau,⁴ G. Chiefari,²⁹ L. Cifarelli,³⁸ F. Cindolo,¹⁰ C. Civinini,¹⁶ I. Clare,¹⁵ R. Clare,¹⁵ G. Coignet,⁴ A.P. Colijn,² N. Colino,²⁶ S. Costantini,⁹ F. Cotorobai,¹³ B. de la Cruz,²⁶ A. Csilling,¹⁴ T.S. Dai,¹⁵ J.A. van Dalen,³¹ R.D' Alessandri,¹⁶ R. de Asmundis,²⁹ P. Deglon,¹⁹ A. Degré,⁴ K. Deiters,⁴⁶ D. della Volpe,²⁹ P. Denes,³⁵ F. DeNotaristefani,³⁶ A. De Salvo,⁴⁸ M. Diemoz,³⁶ D. van Dierendonck,² F. Di Lodovico,⁴⁸ C. Dionisi,^{17,36} M. Dittmar,⁴⁸ A. Dominguez,³⁹ A. Doria,²⁹ M.T. Dova,^{18,4} D. Duchesneau,⁴ D. Dufournand,⁴ P. Duinker,² I. Duran,⁴⁰ S. Easo,³³ H. El Mamouni,²⁵ A. Engler,³⁴ F.J. Eppling,¹⁵ F.C. Erné,² P. Extermann,¹⁹ M. Fabre,⁴⁶ R. Faccini,³⁶ M.A. Falagan,²⁶ S. Falciano,³⁶ A. Favara,¹⁶ J. Fay,²⁵ O. Fedin,³⁷ M. Felcini,⁴⁸ T. Ferguson,³⁴ F. Ferroni,³⁶ H. Fesefeldt,¹ E. Fiandrini,³³ J.H. Field,¹⁹ F. Filt'haut,¹⁷ P.H. Fisher,¹⁵ I. Fisk,³⁹ G. Forconi,¹⁵ L. Fredj,¹⁹ K. Freudenreich,⁴⁸ C. Furetta,²⁷ Yu. Galaktionov,^{28,15} S.N. Ganguli,¹¹ P. Garcia-Abia,⁶ M. Gataullin,³² S.S. Gau,¹² S. Gentile,³⁶ N. Gheordanescu,¹³ S. Giagu,³⁶ S. Goldfarb,²² Z.F. Gong,²⁰ G. Gratta,³⁰ M.W. Gruenewald,⁹ R. van Gulik,² V.K. Gupta,³⁵ A. Gurtu,¹¹ L.J. Gutay,⁴⁵ D. Haas,⁶ B. Hartmann,¹ A. Hasan,³² D. Hatzifotiadou,¹⁰ T. Hebbeker,⁹ A. Hervé,¹⁷ P. Hidas,¹⁴ J. Josa-Mutuberría,²⁶ A. Kasser,²² R.A. Khan,¹⁸ D. Kamrad,⁴⁷ J.S. Kapustinsky,²⁴ M. Kaur,^{18,4} M.N. Kienzle-Focacci,¹⁹ D. Kim,³⁶ D.H. Kim,⁴² J.K. Kim,⁴² S.C. Kim,⁴² W.W. Kinnison,²⁴ A. Kirkby,³² D. Kirkby,³² J. Kirkby,¹⁷ D. Kiss,¹⁴ W. Kittel,³¹ A. Klimentov,^{15,28} A.C. König,³¹ A. Kopp,⁴⁷ I. Korolko,²⁸ V. Koutsenko,^{15,28} R.W. Kraemer,³⁴ W. Krenz,¹ A. Kunin,^{15,28} P. Lacentre,^{47,4,4} P. Ladron de Guevara,²⁶ I. Laktineh,²⁵ G. Landi,¹⁶ C. Lapointe,¹⁵ K. Lassila-Perini,⁴⁸ P. Laurikainen,²¹ A. Lavorato,³⁸ M. Lebeau,¹⁷ A. Lebedev,¹⁵ P. Lebrun,²⁵ P. Lecomte,⁴⁸ P. Lecoq,¹⁷ P. Le Coultre,⁴⁸ H.J. Lee,⁹ J.M. Le Goff,¹⁷ R. Leiste,⁴⁷ E. Leonardi,³⁶ P. Levchenko,³⁷ C. Li,²⁰ C.H. Lin,⁵⁰ W.T. Lin,⁵⁰ F.L. Linde,^{2,17} L. Lista,²⁹ Z.A. Liu,⁸ W. Lohmann,⁴⁷ E. Longo,³⁶ W. Lu,³² Y.S. Lu,⁸ K. Lübelmeyer,¹ C. Luci,^{17,36} D. Luckey,¹⁵ L. Luminari,³⁶ W. Lustermaier,²⁰ W.G. Ma,²⁰ M. Maiti,¹¹ G. Majumder,¹¹ L. Malgeri,¹⁷ A. Malinin,²⁸ C. Mañá,²⁶ D. Mangeol,³¹ P. Marchesini,⁴⁸ G. Marian,^{43,4} J.P. Martin,²⁵ F. Marzano,³⁶ G.G.G. Massaro,² K. Mazumdar,¹¹ R.R. McNeil,³ S. Mele,¹⁷ L. Merola,² M. Meschini,¹⁶ W.J. Metzger,³¹ M. von der Mey,¹ Y. Mi,²² D. Migani,¹⁰ A. Mihul,¹³ H. Milcent,¹⁷ G. Mirabelli,³⁶ J. Mnich,¹⁷ P. Molnar,⁹ B. Monteleoni,¹⁶ T. Moulik,¹¹ R. Mount,³² G.S. Muanza,²⁵ F. Muheim,¹⁹ A.J.M. Muijs,² S. Nahn,¹⁵ M. Napolitano,²⁹ F. Nessi-Tedaldi,⁴⁸ H. Newman,³² T. Niessen,¹ A. Nippe,²² A. Nisati,³⁶ H. Nowak,⁴⁷ Y.D. Oh,⁴² G. Organtini,³⁶ R. Ostonen,²¹ C. Palomares,²⁶ D. Pandoulas,¹ S. Paoletti,^{36,17} P. Paolucci,²⁹ H.K. Park,³⁴ I.H. Park,⁴² G. Pascale,³⁶ G. Passaleva,¹⁷ S. Patricelli,²⁹ T. Paul,¹² M. Pauluzzi,³³ C. Paus,¹⁷ F. Pauss,⁴⁸ D. Peach,¹⁷ M. Pedace,³⁶ Y.J. Pei,¹ S. Pensotti,²⁷ D. Perret-Gallix,⁴ B. Petersen,³¹ S. Petrak,⁹ A. Pevsner,⁵ D. Piccolo,²⁹ M. Pieri,¹⁶ P.A. Piroué,³⁵ E. Pistolesi,²⁷ V. Plyaskin,²⁸ M. Pohl,⁴⁸ V. Pojidaev,^{28,16} H. Postema,¹⁵ J. Pot'her,¹⁷ N. Produit,¹⁹ D. Prokofiev,³⁷ J. Quartier,³⁸ G. Rahal-Callot,⁴⁸ N. Raja,¹¹ P.G. Rancoita,²⁷ M. Rattaggi,²⁷ G. Raven,³⁹ P. Razis,³⁰ D. Ren,⁴⁸ M. Rescigno,³⁶ S. Reucroft,¹² T. van Rhee,⁴⁴ S. Riemann,⁴⁷ K. Riles,³ A. Robohm,⁴⁸ J. Rodin,⁴³ B.P. Roe,³ L. Romero,²⁶ S. Rosier-Lees,⁴ Ph. Rosset,²² S. Roth,¹ J.A. Rubio,¹⁷ D. Ruschmeier,⁹ H. Rykaczewski,⁴⁸ S. Sakai,³⁶ J. Salicio,¹⁷ E. Sanchez,²⁶ M.P. Sanders,³¹ M.E. Sarakinos,²¹ C. Schäfer,¹ V. Schegelsky,³⁷ S. Schmidt-Kaerst,¹ D. Schmitz,¹ N. Scholz,⁴⁸ H. Schopper,⁴⁹ D.J. Schotanus,³¹ J. Schwenke,¹ G. Schwering,¹ C. Sciacca,²⁹ D. Sciarrino,¹⁹ L. Servoli,³³ S. Shevchenko,³² N. Shivarov,⁴¹ V. Shoutko,²⁸ J. Shukla,²⁴ E. Shumilov,²⁸ A. Shvorob,³² T. Siedenb'urg,¹ D. Son,⁴² B. Smith,¹⁵ P. Spillantini,¹⁶ M. Steuer,¹⁵ D.P. Stickland,³⁵ A. Stone,⁷ H. Stone,³⁵ B. Stoyanov,⁴¹ A. Straessner,¹ K. Sudhakar,¹¹ G. Sultanov,¹⁸ L.Z. Sun,²⁰ H. Suter,⁴⁸ J.D. Swain,¹⁸ Z. Szillasi,^{43,4} X.W. Tang,⁸ L. Tauscher,⁶ L. Taylor,¹² C. Timmermans,³¹ Samuel C.C. Ting,¹⁵ S.M. Ting,¹⁵ S.C. Tonwar,¹¹ J. Tóth,¹⁴ C. Tully,³⁵ K.L. Tung,⁸ Y. Uchida,¹⁵ J. Ulbricht,⁴⁸ E. Valente,³⁶ G. Vesztergombi,¹⁴ I. Vetlitsky,²⁸ G. Viertel,⁴⁸ S. Villa,¹² M. Vivargent,⁴ S. Vlachos,⁶ H. Vogel,³⁴ H. Vogt,⁴⁷ I. Vorobiev,^{17,28} A.A. Vorobyov,³⁷ A. Vorvolakos,³⁰ M. Wadhwa,⁶ W. Wallraff,¹ J.C. Wang,¹⁵ X.L. Wang,²⁰ Z.M. Wang,²⁰ A. Weber,¹ S.X. Wu,¹⁵ S. Wynhoff,¹ Z.Z. Xu,²⁰ B.Z. Yang,²⁰ C.G. Yang,⁸ H.J. Yang,⁸ M. Yang,⁸ J.B. Ye,²⁰ S.C. Yeh,⁵¹ J.M. You,³⁴ An. Zalite,³⁷ Yu. Zalite,³⁷ P. Zemp,⁴⁸ Y. Zeng,¹ Z.P. Zhang,²⁰ G.Y. Zhu,⁸ R.Y. Zhu,³² A. Zichichi,^{10,17,18} F. Ziegler,⁴⁷ G. Zilizi,^{43,4}

- 1 I. Physikalisches Institut, RWTH, D-52056 Aachen, FRG[§]
III. Physikalisches Institut, RWTH, D-52056 Aachen, FRG[§]
 - 2 National Institute for High Energy Physics, NIKHEF, and University of Amsterdam, NL-1009 DB Amsterdam, The Netherlands
 - 3 University of Michigan, Ann Arbor, MI 48109, USA
 - 4 Laboratoire d'Annecy-le-Vieux de Physique des Particules, LAPP, IN2P3-CNRS, BP 110, F-74941 Annecy-le-Vieux CEDEX, France
 - 5 Johns Hopkins University, Baltimore, MD 21218, USA
 - 6 Institute of Physics, University of Basel, CH-4056 Basel, Switzerland
 - 7 Louisiana State University, Baton Rouge, LA 70803, USA
 - 8 Institute of High Energy Physics, IHEP, 100039 Beijing, China[△]
 - 9 Humboldt University, D-10099 Berlin, FRG[§]
 - 10 University of Bologna and INFN-Sezione di Bologna, I-40126 Bologna, Italy
 - 11 Tata Institute of Fundamental Research, Bombay 400 005, India
 - 12 Northeastern University, Boston, MA 02115, USA
 - 13 Institute of Atomic Physics and University of Bucharest, R-76900 Bucharest, Romania
 - 14 Central Research Institute for Physics of the Hungarian Academy of Sciences, H-1525 Budapest 114, Hungary[‡]
 - 15 Massachusetts Institute of Technology, Cambridge, MA 02139, USA
 - 16 INFN Sezione di Firenze and University of Florence, I-50125 Florence, Italy
 - 17 European Laboratory for Particle Physics, CERN, CH-1211 Geneva 23, Switzerland
 - 18 World Laboratory, FBLJA Project, CH-1211 Geneva 23, Switzerland
 - 19 University of Geneva, CH-1211 Geneva 4, Switzerland
 - 20 Chinese University of Science and Technology, USTC, Hefei, Anhui 230 029, China[△]
 - 21 SEFT, Research Institute for High Energy Physics, P.O. Box 9, SF-00014 Helsinki, Finland
 - 22 University of Lausanne, CH-1015 Lausanne, Switzerland
 - 23 INFN-Sezione di Lecce and Università Degli Studi di Lecce, I-73100 Lecce, Italy
 - 24 Los Alamos National Laboratory, Los Alamos, NM 87544, USA
 - 25 Institut de Physique Nucléaire de Lyon, IN2P3-CNRS, Université Claude Bernard, F-69622 Villeurbanne, France
 - 26 Centro de Investigaciones Energéticas, Medioambientales y Tecnológicas, CIEMAT, E-28040 Madrid, Spain^b
 - 27 INFN-Sezione di Milano, I-20133 Milan, Italy
 - 28 Institute of Theoretical and Experimental Physics, ITEP, Moscow, Russia
 - 29 INFN-Sezione di Napoli and University of Naples, I-80125 Naples, Italy
 - 30 Department of Natural Sciences, University of Cyprus, Nicosia, Cyprus
 - 31 University of Nijmegen and NIKHEF, NL-6525 ED Nijmegen, The Netherlands
 - 32 California Institute of Technology, Pasadena, CA 91125, USA
 - 33 INFN-Sezione di Perugia and Università Degli Studi di Perugia, I-06100 Perugia, Italy
 - 34 Carnegie Mellon University, Pittsburgh, PA 15213, USA
 - 35 Princeton University, Princeton, NJ 08544, USA
 - 36 INFN-Sezione di Roma and University of Rome, "La Sapienza", I-00185 Rome, Italy
 - 37 Nuclear Physics Institute, St. Petersburg, Russia
 - 38 University and INFN, Salerno, I-84100 Salerno, Italy
 - 39 University of California, San Diego, CA 92093, USA
 - 40 Dept. de Física de Partículas Elementales, Univ. de Santiago, E-15706 Santiago de Compostela, Spain
 - 41 Bulgarian Academy of Sciences, Central Lab. of Mechatronics and Instrumentation, BU-1113 Sofia, Bulgaria
 - 42 Center for High Energy Physics, Adv. Inst. of Sciences and Technology, 305-701 Taejeon, Republic of Korea
 - 43 University of Alabama, Tuscaloosa, AL 35486, USA
 - 44 Utrecht University and NIKHEF, NL-3584 CB Utrecht, The Netherlands
 - 45 Purdue University, West Lafayette, IN 47907, USA
 - 46 Paul Scherrer Institut, PSI, CH-5232 Villigen, Switzerland
 - 47 DESY-Institut für Hochenergiephysik, D-15738 Zeuthen, FRG
 - 48 Eidgenössische Technische Hochschule, ETH Zürich, CH-8093 Zürich, Switzerland
 - 49 University of Hamburg, D-22761 Hamburg, FRG
 - 50 National Central University, Chung-Li, Taiwan, China
 - 51 Department of Physics, National Tsing Hua University, Taiwan, China
- [§] Supported by the German Bundesministerium für Bildung, Wissenschaft, Forschung und Technologie
[‡] Supported by the Hungarian OTKA fund under contract numbers T019181, F023259 and T024011.
[¶] Also supported by the Hungarian OTKA fund under contract numbers T22238 and T026178.
^b Supported also by the Comisión Interministerial de Ciencia y Tecnología.
[‡] Also supported by CONICET and Universidad Nacional de La Plata, CC 67, 1900 La Plata, Argentina.
[‡] Supported by Deutscher Akademischer Austauschdienst.
[◇] Also supported by Panjab University, Chandigarh-160014, India.
[△] Supported by the National Natural Science Foundation of China.

References

- [1] S.L. Glashow, Nucl. Phys. **22** (1961) 579; S. Weinberg, Phys. Rev. Lett. **19** (1967) 1264; A. Salam, “Elementary Particle Theory”, Ed. N. Svartholm, Stockholm, “Almqvist and Wiksell” (1968), 367.
- [2] M. Consoli and W. Hollik, in “Z Physics at LEP 1”, CERN Report CERN 89-08 Vol.1, 7; M. Böhm and W. Hollik, in “Z Physics at LEP 1”, CERN Report CERN 89-08 Vol.1, 203.
- [3] L3 Collab., B. Adeva *et al.*, Nucl. Instr. and Meth. **A 289** (1990) 35; M. Acciarri *et al.*, Nucl. Instr. and Meth. **A 351** (1994) 300; I.C. Brock *et al.*, Nucl. Instr. and Meth. **A 381** (1996) 236; A. Adam *et al.*, Nucl. Instr. and Meth. **A 383** (1996) 342.
- [4] L3 Collab., M. Acciarri *et al.*, Phys. Lett. **B 335** (1994) 542.
- [5] L3 Collab., M. Acciarri *et al.*, Measurement of the Effective Weak Mixing Angle by Jet–Charge Asymmetry in Hadronic Decays of the Z Boson, Submitted to Phys. Lett.
- [6] ALEPH Collab., D. Buskulic *et al.*, Phys. Lett. **B 384** (1996) 414.
- [7] DELPHI Collab., P. Abreu *et al.*, Z. Phys. **C 65** (1995) 569; DELPHI Collab., P. Abreu *et al.*, Phys. Lett. **B 332** (1994) 488.
- [8] OPAL Collab., R. Akers *et al.*, Z. Phys. **C 67** (1995) 365.
- [9] L3 Collab., B. Adeva *et al.*, Phys. Lett. **B 252** (1990) 703.
- [10] L3 Collab., B. Adeva *et al.*, Phys. Lett. **B 288** (1992) 395.
- [11] T. Sjöstrand, Comp. Phys. Comm. **39** (1986) 347; T. Sjöstrand and M. Bengtsson, Comp. Phys. Comm. **43** (1987) 367.
- [12] The L3 detector simulation is based on GEANT Version 3.15. R. Brun *et al.*, “GEANT 3”, CERN DD/EE/84-1 (Revised), September 1987. The GHEISHA program (H. Fesefeldt, RWTH Aachen Report PITHA 85/02 (1985)) is used to simulate hadronic interactions.
- [13] ALEPH,DELPHI,L3 and OPAL Collaborations, Nucl. Instr. and Meth. **A 378** (1996) 101.
- [14] ALEPH,DELPHI,L3,OPAL and SLD Collaborations, Input Parameters for the LEP/SLD Electroweak Heavy Flavour Results for Summer 1998 Conferences, in preparation.
- [15] C. Peterson *et al.*, Phys. Rev. **D 27** (1983) 105.
- [16] G. Altarelli *et al.*, Nucl. Phys. **B 208** (1982) 365.
- [17] N. Isgur *et al.*, Phys. Rev. **D 39** (1989) 799.
- [18] DELCO Collab., W. Bacino *et al.*, Phys. Rev. Lett. **43** (1979) 1073.
- [19] MARK III Collab., R.M. Baltrusaitis *et al.*, Phys. Rev. Lett. **54** (1985) 1976.

- [20] CLEO Collab., D. Bortoletto *et al.*, Phys. Rev. **D 45** (1992) 21.
- [21] The Particle Data Group, C. Caso *et al.*, Eur. Phys. J. **C3** (1998) 1.
- [22] D. Bardin *et al.*, Phys. Lett. **B 255** (1991) 290.
- [23] D. Abbaneo *et al.*, Eur. Phys. J. **C4** (1998) 185.
S.C. Blyth, L3 Internal note 2181 (1997). ¹⁾

¹⁾L3 Internal Notes are freely available upon request from
The L3 Secretariat, CERN, CH-1211 Geneva 23, Switzerland.
Internet: <http://l3www.cern.ch>.

Category (k)	μ	e	A_k
$b \rightarrow \ell^-$	62.7	74.7	A_b
$b \rightarrow c \rightarrow \ell^+$	7.5	5.8	$-A_b$
$b \rightarrow \tau \rightarrow \ell^-$	0.9	1.1	A_b
$b \rightarrow \bar{c} \rightarrow \ell^-$	1.1	0.6	A_b
$c \rightarrow \ell^+$	10.0	6.1	$-A_c$
background	17.8	11.7	A_{bkg}

Table 1: Monte Carlo estimates of the composition (%) of the single lepton data sample and the corresponding asymmetry contributions.

Category	$\mu\mu$	ee	μe	$\ell\ell$
$b \rightarrow \ell, b \rightarrow \ell$	66.0	75.6	72.6	70.3
$b \rightarrow \ell, b \rightarrow c \rightarrow \ell$	17.4	13.6	13.9	15.3
$b \rightarrow \ell, b \rightarrow \text{background}$	7.2	4.8	7.9	7.2
$b \rightarrow c \rightarrow \ell, b \rightarrow \text{background}$	1.3	0.4	4.4	0.8
$b \rightarrow c \rightarrow \ell, b \rightarrow c \rightarrow \ell$	0.7	0.7	0.3	0.5
$b \rightarrow \text{background}, b \rightarrow \text{background}$	0.1	0.4	0.2	0.2
$c \rightarrow \ell, c \rightarrow \ell$	2.4	0.4	0.7	1.3
others	4.8	4.1	3.9	4.3

Table 2: Monte Carlo composition (%) estimates for the dilepton sample. ‘Others’ refers to misidentified hadrons or leptons from light hadron decays. The $b \rightarrow \ell$ fraction includes $b \rightarrow \tau \rightarrow \ell$ and $b \rightarrow \bar{c} \rightarrow \ell$ decays.

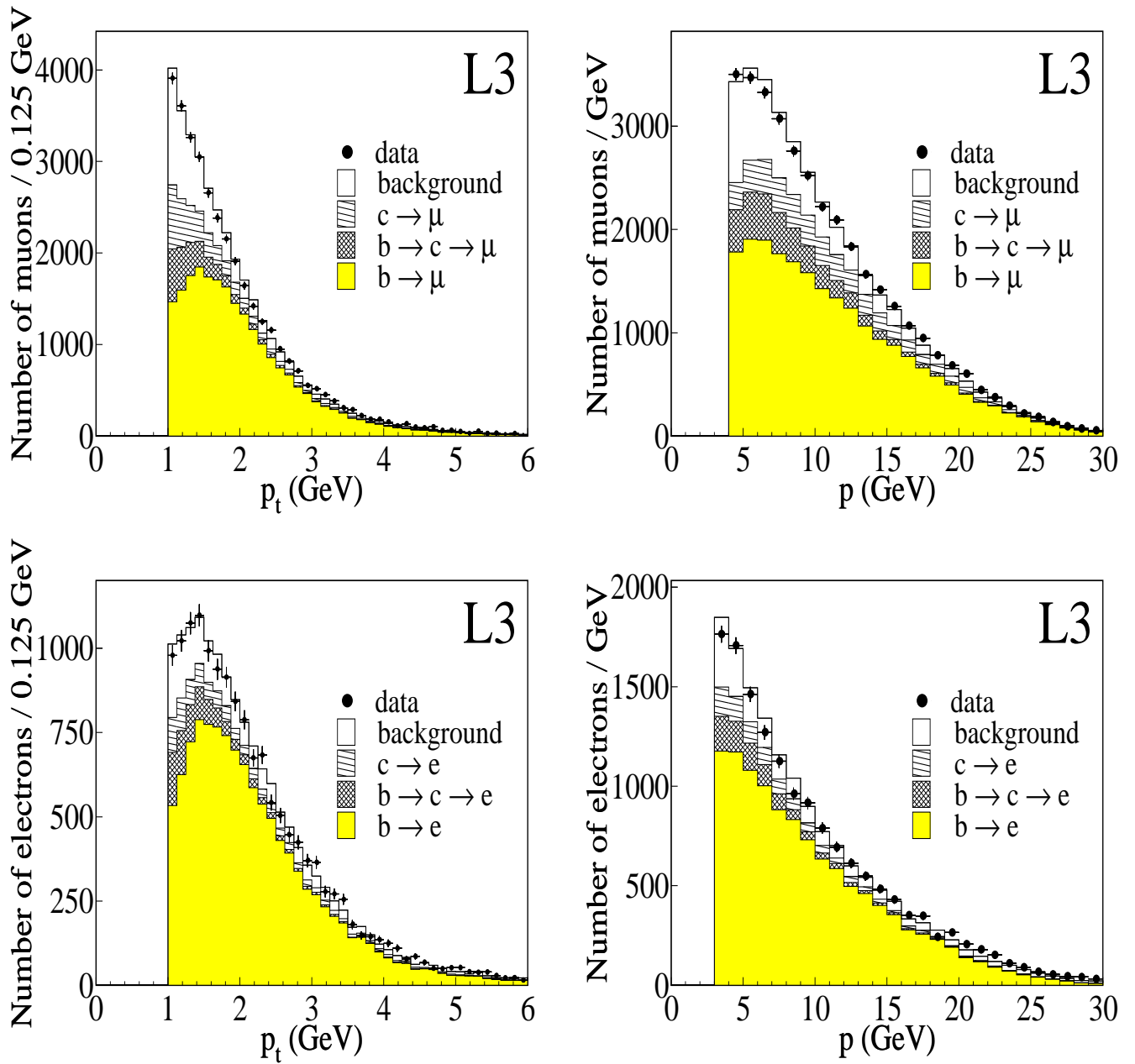


Figure 1: The p_t and p distributions for muons and electrons, with Monte Carlo expectations of contributions from various sources.

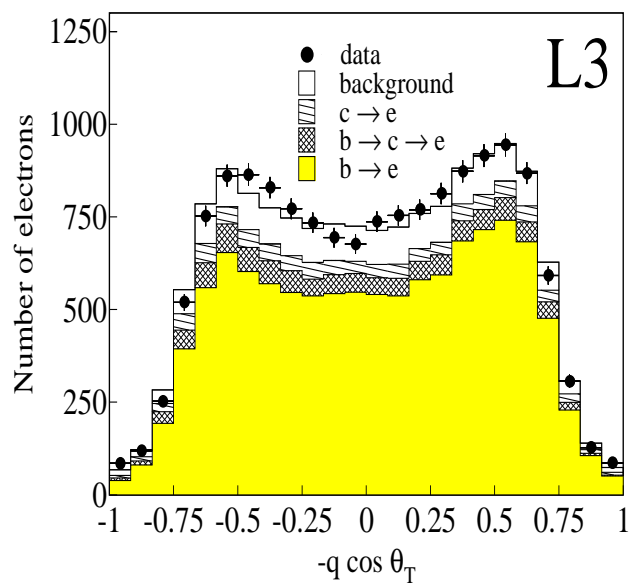
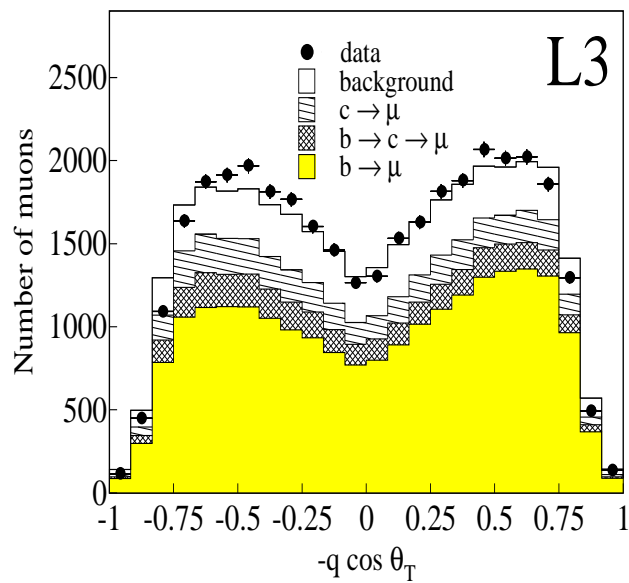


Figure 2: The $-q \cos \theta_T$ distributions for muons and electrons, with Monte Carlo expectations of contributions from various sources.

Contribution	Value & Variation	$\Delta\chi_b$ $\times 10^2$	$\Delta A_{\text{FB}}^{\text{obs}}$ $\times 10^2$	$\Delta A_{\text{FB}}^{\text{b}}$ $\times 10^2$
R_b	0.2170 ± 0.0009	+0.000	-0.008	-0.010
R_c	0.1734 ± 0.0048	+0.001	+0.032	+0.042
A_c^{FB}	0.0741 ± 0.0048	+0.000	+0.051	+0.067
Electroweak Parameters		0.001	0.061	0.079
$\langle x_{\text{E}}(\text{b}) \rangle$	0.7020 ± 0.0080	+0.000	+0.004	+0.005
$\langle x_{\text{E}}(\text{c}) \rangle$	0.4840 ± 0.0080	+0.000	+0.017	+0.023
$\text{Br}(\text{b} \rightarrow \ell)$	0.1050 ± 0.0050	+0.262	-0.122	-0.092
$\text{Br}(\text{b} \rightarrow \text{c} \rightarrow \ell^+)$	0.0800 ± 0.0050	-0.291	+0.049	-0.010
$\text{Br}(\text{b} \rightarrow \bar{\text{c}} \rightarrow \ell^-)$	0.0162 ± 0.0040	+0.063	-0.017	-0.006
$\text{Br}(\text{b} \rightarrow \tau \rightarrow \ell)$	0.0045 ± 0.0008	+0.000	-0.008	-0.010
$\text{Br}(\text{c} \rightarrow \ell)$	0.0980 ± 0.0050	+0.003	+0.055	+0.073
$\text{Br}(\text{b} \rightarrow \text{J}/\psi \rightarrow \ell\ell)$	0.0007 ± 0.0002	+0.000	+0.023	+0.030
Fragmentation and Branching Ratios		0.397	0.147	0.124
$\text{b} \rightarrow \ell$ model		-0.030	-0.046	-0.067
$\text{c} \rightarrow \ell$ model		-0.186	+0.116	+0.104
$\text{b} \rightarrow \text{D}$ model		-0.153	+0.022	-0.010
Decay Models		0.243	0.127	0.125
background fraction	1.0000 ± 0.1000	-0.001	+0.049	+0.063
background asymmetry	0.0000 ± 0.0100	+0.000	-0.166	-0.217
Background effects		0.001	0.173	0.226
charge confusion correction		-0.097	+0.013	-0.008
lepton-jet angle smearing	1°	+0.138	+0.108	+0.145
lepton momentum smearing	2%	+0.011	+0.017	+0.023
Detector effects		0.169	0.110	0.147
α, β, B	$\pm 2\%$	+0.132	+0.000	+0.034
Mixing specific uncertainties		0.132	0.000	0.034
Total Systematic		0.512	0.289	0.334

Table 3: Systematic uncertainties on χ_b , $A_{\text{FB}}^{\text{obs}}$ and A_{FB}^{b} for muons and electrons collected during the 1993-95 peak running periods, $\langle\sqrt{s}\rangle = 91.24$ GeV.

\sqrt{s} (GeV)	A_{FB}^{b}
89.50	$0.0611 \pm 0.0293 \pm 0.0043$
91.26	$0.0980 \pm 0.0067 \pm 0.0034$
93.10	$0.1371 \pm 0.0240 \pm 0.0044$

Table 4: A_{FB}^{b} for different centre-of-mass energies after applying QCD corrections. These results are from the full LEP1 data, with statistical and systematic uncertainties provided.

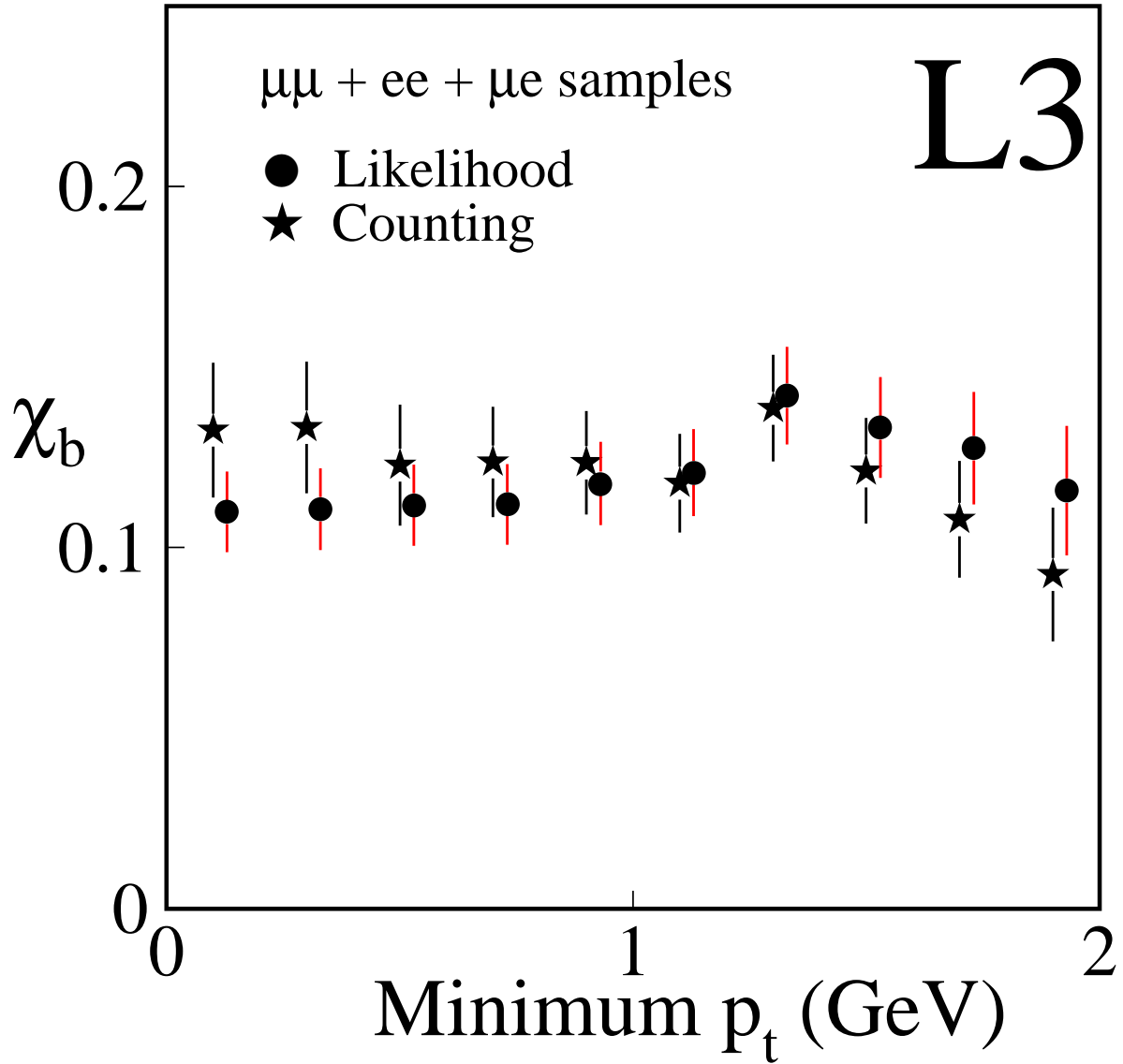


Figure 3: Mixing parameter values as a function of the minimum transverse momentum for the factorized fit method (dots) and a simple counting method (stars). The dots are displaced horizontally for improved visibility.

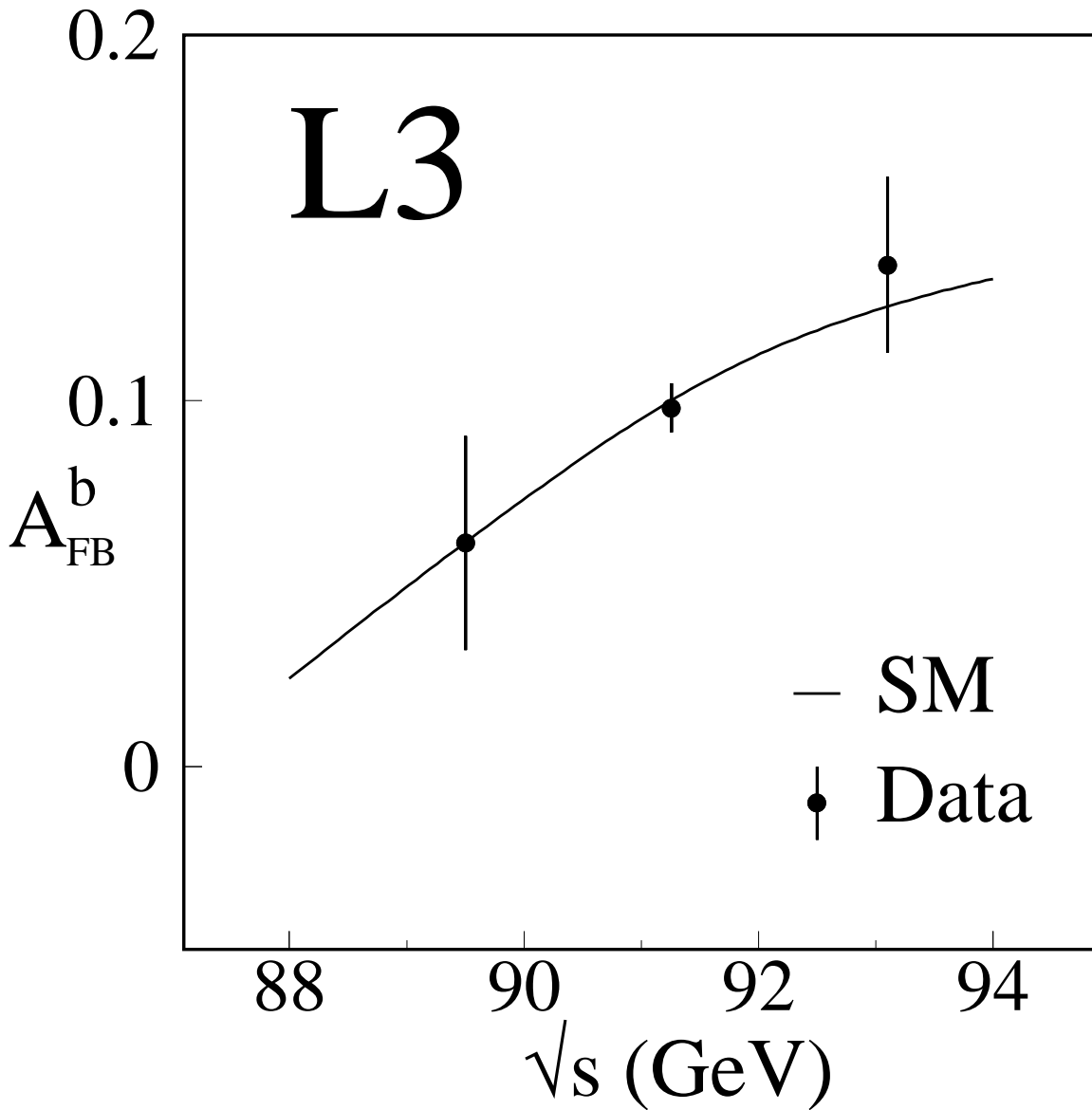


Figure 4: The energy dependence of A_{FB}^b , after QCD correction, is compared with the Standard Model predictions of ZFITTER with QCD effects removed, corresponding to $\sin^2 \bar{\theta}_W = 0.2315$.